DESIGN OF A 3.5 T SUPERCONDUCTING MULTIPOLE WIGGLER

J. C. Jan[†], H. H. Chen, S. D. Chen, F. Y. Lin, C. S. Hwang, C. H. Chang, T. Y. Chung, G. H. Luo,
National Synchrotron Radiation Research Center, Hsinchu, Taiwan, R.O.C

Abstract

A 3.5 T superconducting multipole wiggler (SMPW) was designed by a collaboration of the National Synchrotron Radiation Research Center (NSRRC) and the Synchrotron Light Research Institute (SLRI). The SMPW will provide hard X-rays for the X-ray absorption spectroscopy (XAS) beamline at the SLRI. The design concept of the SMPW is following and improving on the operating experience of superconducting magnets in the NSRRC. Stable operation, compatible with the cooling capacity in the cryostat, is the main design goal. Fast and safe recovery from a quench event is also desired. The magnetic circuit and mechanical design, stress and heat load analysis of the SMPW are discussed in this paper.

INTRODUCTION

A superconducting magnet can be a useful X-ray source in a low energy storage ring. A collaboration between NSRRC and SLRI has been started to design and construct a 3.5 T SMPW that will be installed in the storage ring of SLRI. The mechanical design was improved based on experience with such magnets in NSRRC to increase the filling period between liquid Helium (LHe) supplies and the stability of the superconducting wire [1,2]. A large cryo-plant and auto-filling system ensures a stable LHe supply in the SMPW cryostat [3]. When the superconducting coil is immersed and cooled in the LHe bath, the required temperature and heat balance is achieved fast. An optimized cryostat thus require to minimize the LHe consumption and safe operating.

MAGNETIC CIRCUIT DESIGN

The magnetic field of the SMPW is designed for 3.5 T in a 22.5 mm gap between poles. A round cross-section NbTi superconducting wire with high current density capability was selected for the magnet coils. A full model of the SMPW was created and simulated by the RADIA software [4]. The model consists of six magnet periods and four end poles as displayed in Fig. 1 (a) and (b). The pole profile and coil windings are of the race-track shape which the simulation parameters and results are listed in Table 1. A peak field of 3.55 T was reached with an excitation current of 257 A. The maximum field of 3.98 T at a current of 297 A is limited by the critical magnetic field on the coil surface. The longitudinal field distribution and transverse field homogeneity of the SMPW are displayed in Fig. 2 (a) and (b). The transverse roll-off is less than 0.15% within ±25 mm. Both, the first field integral (IB_z) determines the SMPW overall electron beam deflection angle as well as the second field integral (IIB_z) for the

beam offset are very close to zero. Figure 3 shows the simulated field strength, inductance and stored energy of the SMPW as a function of excitation current. The total force between upper and lower magnet array is approximate 170 kN.
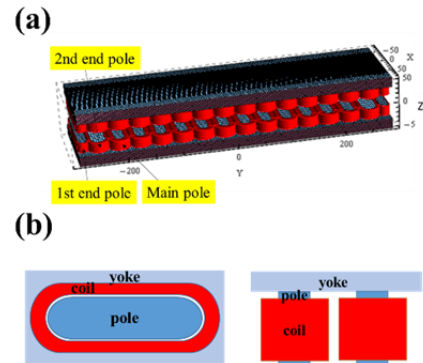
Figure 1: Computer design for the (a) full model with coil and (b) cross section of the SMPW.

Table 1: RADIA Simulation Parameters and Results

Parameters	Nominal
Wire material	NbTi
Pole material	Iron (low carbon steel)
Wire dimension	D0.600 mm (bare) / D0.650 mm(insulated)
Cu/SC ratio	1.30
Peak field strength, B_z	3.55 T @ 257 A
Max. field on conductor, B_s	5.15 T @ 257 A
Period length	77 mm
Number of main periods	6
Pole gap	22.5 mm
Clearance aperture, V×H	15 mm × 106 mm
Deflection parameter, K	25.53 @ 257 A
Radiation fan at 1.2 GeV	±10.8 × ± 0.43 mrad²
Energy	129.1 kJ @ 257 A
Inductance	3.91 H @ 257A
Good field region, ± 25 mm	ΔB/B ≤ 0.15%
IB_z @ I	0 G·cm @ 257 A
IIB_z @ I	-16 G·cm² @ 257 A
Total force on the array	170 kN

Photon spectra were calculated with the IGOR/SRWE program and comparisons between the wavelength shifter (WLS) and the SMPW design are plotted in Fig. 4 [5]. The photon flux from the SMPW at 3.5 T is greater than 1×10^{13} (photon/s/mrad/0.1% bw) and extends to photon energies up to 11 keV.

---

† janjc@nsrrc.org.tw
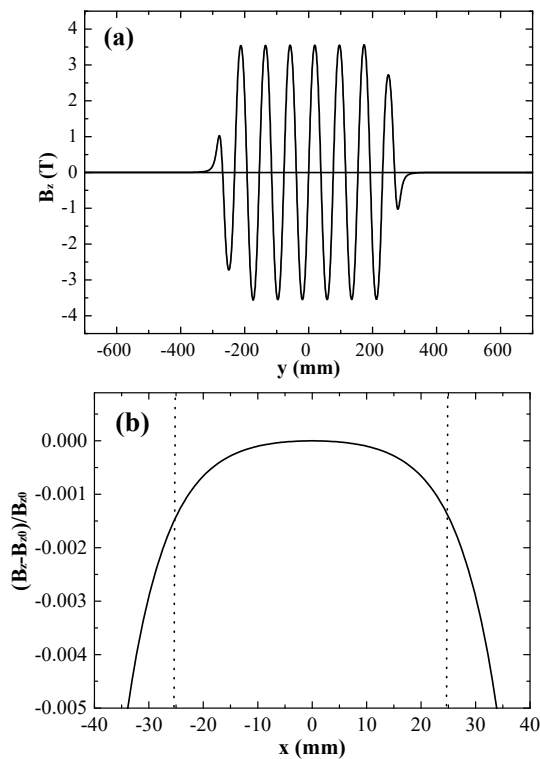
Figure 2: (a) Field distribution along the electron beam direction and (b) field roll-off in the transverse direction.
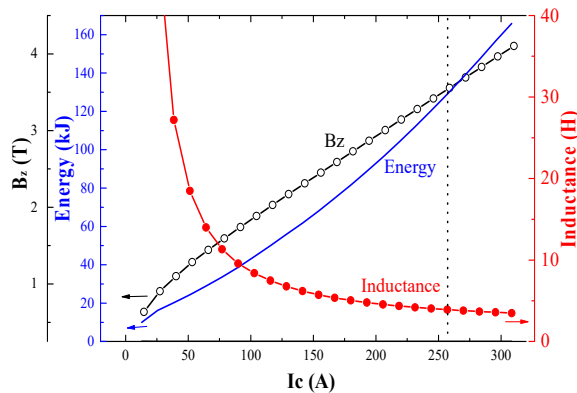
Figure 3: Variation of the field strength, inductance and stored energy as a function of the excitation current.
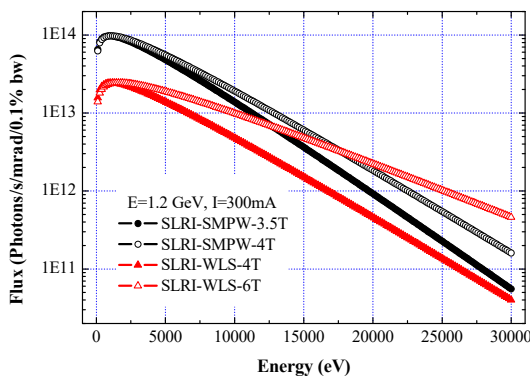
Figure 4: Comparison of radiation spectra between WLS and SMPW.

MECHANICAL DESIGN

The mechanical design of the SMPW includes the magnet array, cryostat, corrector magnet and extended BPM as displayed in Fig. 5 (a).
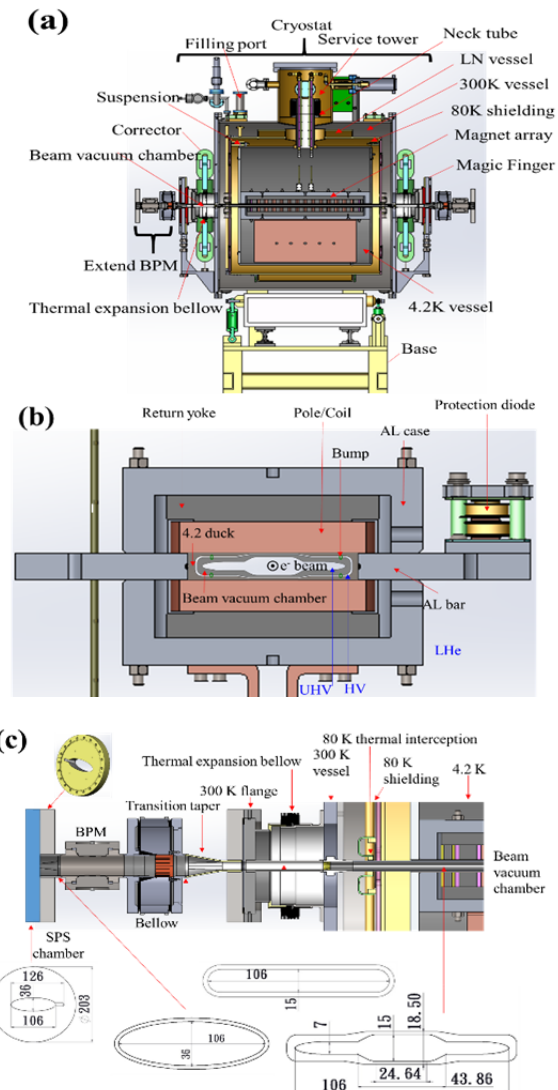
Figure 5: (a) Cryostat of the SMPW, (b) cross-section of the magnet array and (c) transition of the chamber profile.

LHe Vessel

The iron pole, coil and return yoke are sealed and fixed by resin in an aluminum case and called magnet array. An aluminum bar was inserted between upper and lower poles to resist the deformation due to the attractive force and to ensure precise gap dimensions as displayed in Fig. 5 (b). The protection diode is mounted on the aluminum bar thus increasing the capacity of operating LHe compared to a prior design (original diode is mounted on the magnet array), because the lower-level of LHe can be brought down and filling period thus be extended during operation. A 4.2 K duct was inserted between upper and lower array to separate the LHe pressure and high vacuum (HV) in the cryostat. A beam vacuum chamber of aluminum alloy was inserted in the 4.2 K duct to separate the

high vacuum of the cryostat from the ultra-high vacuum (UHV) of the storage ring. The beam vacuum chamber was welded to a 300 K flange via a 80 K thermal interception at both end as displayed in Fig. 5 (c). Twelve FRP bumps (functioning as a spacer) will be installed between the 4.2 K duct and the beam vacuum chamber to avoid physical contact between 4.2 K duct and 90 K beam vacuum chamber. The beam vacuum chamber also helps to decrease the radiation heat from the 300 K vessel into the LHe vessel directly.

80 K Shield and 300 K Vessel

A liquid nitrogen (LN) cooled shielding at 80 K is surrounding the LHe vessel for which the chamber transition profile is shown in Fig. 5 (c). A special suspension system is used between the LHe vessel and the 300 K vessel for support and reduce the heat leakage into the LHe vessel. A safety valve and burst disk will be installed to protect unexpected pressure raises in the LHe vessel.

STRESS ANALYSIS AND HEAT LOAD BUDGET

The stress and heat load of components are simulated by ANSYS software and discussed below [6].

Attracting Magnetic Force on the Iron Poles

The attractive force between the upper and lower magnet arrays is approximately 170 kN according to simulation. The return yoke acts as a strong back to resist any deformation. The total deformation of the iron pole under the attractive force is 0.9 µm.

Stress Analysis of the Beam Chamber and 4.2 K Duct

The 4.2 K duct and beam vacuum chamber are constructed from thin walled material and need to absorb the pressure variation as displayed in Fig. 5 (b). The outside and inside pressure of the beam vacuum chamber is close to vacuum under normal operation, respectively. However, the 300 K vessel and the vacuum chamber have to be vented occasionally to atmospheric pressure during maintenance. The vacuum chamber should therefore resist the deformation and not break under 1 atm of pressure difference across both sides of the wall. The deformation of the vacuum chamber was calculated to be 0.167 mm under 1atm of pressure difference. In addition, the 4.2 K duct separates the LHe and HV regions and should be able to absorb the change in pressure during a coil quench. The maximum deformation of the 4.2 K duct is 0.38 mm at a pressure difference of 30 psi.

Stress Analysis of the Suspension

The weight of the cold mass including the magnet arrays and LHe vessel is about 15 kN including a 3g gravity. The thermal stress of the suspension comes from the suspension itself and from the 4.2 K vessel as it contracts during cool down. The total thermal stress of the suspension is estimated to be about 1.5 mm after cool down. The

limit of elastic deformation for this suspension is approximately 3 mm as measured by a tension test. Thus the suspension is strong enough to resist the thermal contraction.

Heat-Load Budget of the Cryostat

Heat leakage from the 300 K vessel to the LHe/LN vessel is considered and includes conduction, convection and thermal radiation heat transfer. A summary of the cryogenic heat loads are listed in Table 2. The static heat load of the LHe vessel is 1.54 W during magnet excitation. The temperature of the LHe vessel, thermal shielding, vacuum beam chamber and 300 K vessel are set to 4.2, 80, 90 and 300 K in the simulation, respectively. Moreover, the bending magnet power (BMPD) and power from image currents (IMPD) caused by the passing electron current will generate heating. That heat load on the beam vacuum chamber can be easily absorbed by LN.

Table 2: Heat Load Budget of SMPW

Heat load source	Heat load (W)
LHe vessel head load	
Vapor cooled current leads @ 300 A	0.68
Neck tube in the Service tower	0.27
Suspension	0.43
Beam vacuum chamber bump	0.065
Thermal radiation (80 K - 4.2 K)	0.0068
Instrument leads	0.09
Total heat load into LHe vessel	1.54
LN vessel head load	
LN vessel support: 300K-80K	2.12
Thermal transition: to suspension	1.42
Thermal transition: to beam chamber	25.90
Thermal radiation: 300K - 80K	2.01
BMPD	0.098
ICPD	0.112
Total heat load into LN vessel	31.66

SUMMARY

A 3.5 T SMPW was designed by NSRRC and will be installed in SLRI, 2018. Design improvements include an enlarged LHe vessel and rearrangement of the protection diode location thus increasing the filling period time of LHe. The heat leakage into the LHe vessel and LN vessel is 1.54 W and 31.66 W, respectively, after optimization of the cryostat. A challenge is the field measurement within the cryostat. A precise mapping chamber will be designed and inserted in the narrow gap of 90 K beam vacuum chamber. The mapping chamber will provide a room temperature environment to the field measurement sensor.

REFERENCES

[1] C. H. Chang *et al*., "In-achromatic superconducting wiggler in taiwan light source: installation and test results", THPLS139, *EPAC06*, Edinburgh, UK. (2006).

[2] C. S. Hwang *et al.*, "Superconducting wiggler with semi-cold beam duct at Taiwan light source", *Nucl. Instrum. Meth*. A 556, (2006) 607-615.

[3] F. Y. Lin *et al.*, " Auto-filling cryogenic system for super-conducting wiggler", *EPAC04*, Lucerne, Switzerland. (2004) 1726-1728.

[4] P. Elleaume *et al.*,"Computing 3D magnetic field from insertion devices", *Proc. Particle Accelerator Conf. PAC97*, pp. 3509-3511, 1997.

[5] https://www.wavemetrics.com/index.html

[6] ANSYS® Academic Research, Release 14.5 , ANSYS Inc.